PHYSICAL REVIEW A **79**, 041802(R) (2009)

Complexity of two-dimensional quasimodes at the transition from weak scattering to Anderson localization

C. Vanneste* and P. Sebbah
Laboratoire de Physique de la Matière Condensée, CNRS UMR 6622, Université de Nice-Sophia Antipolis, Parc Valrose 06108, Nice, Cedex 02, France
(Received 10 July 2008; published 7 April 2009)

Quasimodes of an open finite-size two-dimensional (2D) random system are computed and systematically characterized in terms of their spatial extension η, complexity factor q^2, and phase distribution for a collection of random systems ranging from weakly scattering to localized systems. A rapid change is seen in η and q^2 at the crossover from localized to diffusive which corresponds to the emergence of 2D extended multipeaked quasimodes analogous to the necklace states recently observed in one dimension. These 2D quasimodes are interpreted in terms of coupled localized states.

DOI: 10.1103/PhysRevA.79.041802 PACS number(s): 42.25.Dd, 42.55.Zz

Transport in random media is driven by the nature of the underlying eigenmodes. Propagation is diffusive when the modes extend spatially, while spectral level overlap occurs in transmission spectra. As the degree of the overlap decreases, transport is inhibited and modes become spatially localized [1]. The theory of Anderson localization predicts a transition between localized and extended eigenstates for spatial dimensions larger than 2 [2]. Renewed interest in the localization transition has been boosted by the active ongoing search for localization of Bose-Einstein condensate in laser speckle fields [3,4], the recent observations of the slowing down of diffusion in ultrasounds [5], microwave [6] and time-resolved optical [7] experiments, and new theoretical progresses [8,9] toward an analytical description of the metal-insulator transition (MIT). The question of the spatial extent of the modes near the Anderson transition is also central in random lasers [10,11]. The threshold may vary by orders of magnitude between localized systems where the modes are spatially confined and diffusive systems where the modes are extended. Besides their spatial extent, another property of the modes in open random media is their complexity. As their spatial extent is increased up to the sample dimensions and their linewidth broadens with increasing leakage through the boundaries, the decaying quasimodes or resonances, which generalize the concept of mode to leaky systems [12], become complex valued, with their standing-wave component being progressively replaced with a component traveling toward the opened boundaries [13]. This is analogous to chaotic cavities with an increasing degree of opening [14]. This is an important aspect rarely addressed in the context of random media.

In this Rapid Communication, we use numerical simulations to explore the nature of the quasimodes of two-dimensional (2D) open random media when scattering strength is increased. The spatial extension of the computed quasimodes, their complexity factor, and their phase distribution are calculated for a statistical ensemble of random configurations for each value of the scattering strength. These quantities reveal the change in regime and the crossover from diffusive to localized. A detailed analysis of the phase probability distribution for each mode shows multipeaked wave functions in the vicinity of the crossover when the localization length is comparable to the sample size. These extended multipeaked quasimodes are interpreted in terms of coupling of localized isolated states, which hybridize to form 2D necklace states.

We consider a two-dimensional random collection of parallel dielectric cylinders with infinite extension, radius $r=60$ nm, and refractive index n embedded in a background matrix of index 1. The volume fraction is $\phi=40\%$ and the system size is $L^2=5\times5\ \mu\text{m}^2$. Maxwell equations for transverse magnetic polarization are modeled using the finite-difference time-domain method [15]. Open boundary conditions are approximated by perfectly matched layer (PML) absorbing boundaries [16]. The index of refraction n is varied from 1.05 to 2.0, in step of 0.05, corresponding to scattering mean-free path ranging from 50 to 0.1 μm. For most of this range, modes are short lived with strong spectral overlap, preventing individual excitation of a mode at its eigenfrequency by a monochromatic source. To obtain the wave function of such short-lived modes, we use recent results [17] which show that, when operating just above threshold, the first lasing mode of an active random system corresponds to a quasimode of the passive system, even in weakly scattering systems where modal overlap dominates. Introducing gain and adjusting the pumping rate just above threshold is therefore an alternative to select a quasimode of the passive cavity. To model the gain, we couple the population equations of a four-level atomic system to the Maxwell equations via the polarization equation [18]. The gain naturally selects the mode with the longest lifetime and the best spectral overlap with the gain curve. All the parameters and initial conditions used here have been already fully described in [19].

We study 150 random configurations, 10 on average per value of refractive index n. The amplitude and phase spatial distributions of the mode are obtained by integrating the in and out of phase oscillating fields over a period. Examples of spatial distributions of the magnitude are shown in Fig. 1 for decreasing values of the refractive index n, illustrating different degrees of spatial extension of the wave functions within the system. The corresponding phase probability dis-

*vanneste@unice.fr

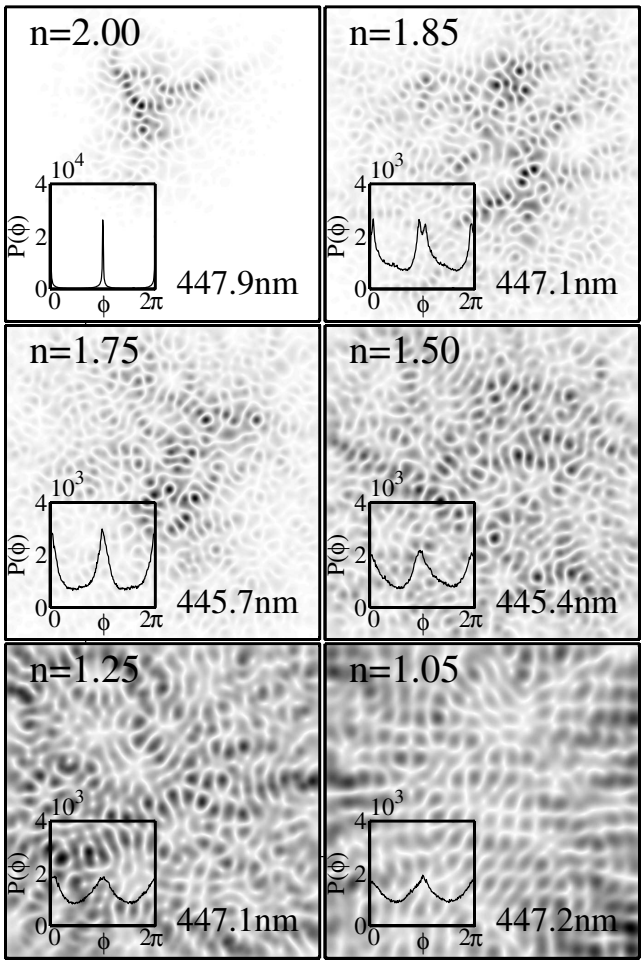

FIG. 1. Spatial distribution and wavelength of quasimodes corresponding to decreasing values of the refractive index of the scatterers; $n=2.00$ to $n=1.05$ (random configurations are not necessarily identical). All modes are in a narrow spectral range around the maximum of the gain curve; $\lambda=446.9$ nm. Each frame shows in inset the phase distribution between 0 and 2π of the corresponding quasimodes. Note the double-peaked distribution for $n=1.85$.

tributions between 0 and 2π are shown in insets in Fig. 1. The phase distribution is peaked around 0 and π when the mode is localized ($n=2$), while it is more uniformly distributed in the extended case. Note that for values of the refractive index as low as 1.05, scattering is weak and the field is rather concentrated at the edges of the system. In that case, residual reflection either at the boundaries or from the PML layers may not be negligible and may result in periodic patterns, similar to those of a Fabry-Perrot cavity, as seen in the bottom-right frame of Fig. 1. We checked that above $n=1.10$, this effect is insignificant and lasing is solely due to multiple scattering within the system.

As the scattering strength is reduced, the spatial expansion of the eigenfunctions increases, as well as their imaginary part resulting from leakage at the open boundaries. To quantify these two characteristics, the quasimodes are described in terms of their spreading factor η and their complexity factor q^2. We define the spreading factor as $\eta=3/L^4\int\int\tilde{A}(\vec{r})\tilde{A}(\vec{r}')|\vec{r}-\vec{r}'|^2d^2\vec{r}d^2\vec{r}'$, where the field amplitude $A(\vec{r})$ is normalized, $\tilde{A}(\vec{r})=A(\vec{r})/[\int\int A^2(\vec{r})d^2\vec{r}]^{1/2}$. The normalizing factor $3/L^4$ ensures that η is unity for uniform distribution of the field amplitude. It measures the degree of spatial extension of the energy within the system alike the participation ratio for instance. However, due to the weighting factor $|\vec{r}-\vec{r}'|^2$, it also enables us to distinguish systems with spatial localization of energy inside the system, as in Fig. 1 for $n=2$, from concentration of energy at the boundaries of the system, as in Fig. 1 for $n=1.05$. Indeed, it can be less than 1 for spatially localized modes or larger than 1 when energy is distributed near the system edges. This is reminiscent of distributed feedback lasers [20] where, in the overcoupled regime (corresponding to $\eta<1$), energy is concentrated inside the laser as a result of strong feedback from scatterers, while in the undercoupled regime ($\eta>1$), energy is concentrated at the edges since the lasing modes result from scattering at the boundaries in order to maximize the gain volume [21]. The complexity factor $q^2=\langle \mathrm{Im}(\Psi)^2\rangle/\langle \mathrm{Re}(\Psi)^2\rangle$ [22] or equivalently the phase rigidity $\rho=(1-q^2)/(1+q^2)$ [23] were introduced in the field of quantum chaos to quantify the degree of complexity of the eigenmode $\Psi(\vec{r})=A(\vec{r})e^{i\phi(\vec{r})}$ and the mutual influence of neighboring resonances [24]. The complexity factor varies from 0 for real standing-wave functions—corresponding to a phase distribution peaked at 0 and π—to 1 for purely traveling waves—corresponding to a flat phase distribution. To the best of our knowledge, it has never been used as a probe to characterize the crossover from localized to extended states in finite disordered systems.

The spreading factor and the complexity factor are computed for each mode and averaged over sample configurations for each value of n. They are shown in Fig. 2 as a function of the scattering mean-free path ℓ calculated using Mie theory for infinite cylinders of refractive index n. The complexity factor increases with the mean-free path, which means that the traveling-wave component replaces progressively the standing-wave component of the mode. While the complexity factor explores values between 0.06 and 0.78, it shows clearly two different regimes, with a crossover around $\ell=0.14$ μm corresponding to $n=1.8$. A transition occurs around the same value of ℓ for the spreading factor, which ranges between 0.16 and 1.23. This particular value of n certainly is not universal and depends on the sample size, but it should correspond to a localization length ξ on the order of the sample size. We confirm this hypothesis by calculating ξ directly from the value of the lasing threshold averaged over sample realizations $\langle P\rangle$. Indeed, the spectral width of the modes Γ, resulting from leakage at the boundaries is given by $\Gamma=\Gamma_0\exp(-L/\xi)$ [25]. It is also directly proportional to the lasing threshold P, since at threshold losses are compensated by gain. Therefore $\xi=L/(\ln\langle P_0\rangle-\ln\langle P\rangle)$, where $\langle P\rangle$ designates the average over sample configurations for each value of n and $\ln\langle P_0\rangle=20.15$ is obtained by extrapolating $\langle P\rangle$ at $n=1$. The dependence of ξ on refractive index n is shown in the inset in Fig. 2 and is compared to the theoretical expression in the limit of independent scattering, as given in [25] by $\xi_{\mathrm{th}}=\ell\exp[\pi\,\mathrm{Re}(k_{\mathrm{eff}})\ell/2]$, where ℓ is the mean-free path and k_{eff} is the effective wave number. Both curves (full lines in inset of Fig. 2) approach in the crossover region

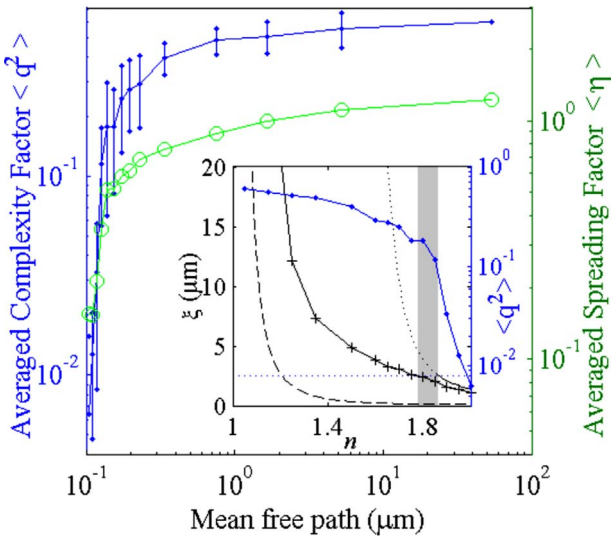

FIG. 2. (Color online) Complexity factor (dots) q^2 and spreading factor (circles) η averaged over sample configuration versus scattering mean-free path ℓ. The fluctuations around the average $\pm\langle q^2-\langle q^2\rangle\rangle^{1/2}$ are represented by the bars. Inset: averaged complexity factor q^2 (dots) and localization length ξ versus index of refraction n calculated from the averaged lasing threshold (crosses) and from independent scattering theory [full line where relevant ($\xi \leq L/2$); dotted line otherwise]. The dashed line represents the mean-free path ℓ. The horizontal dotted line corresponds to $\xi=L/2$.

around $n=1.8$, which corresponds to $\xi \sim L/2=2.5$ μm, where the two expressions for ξ and ξ_{th} start to be valid [26].

Also shown in Fig. 2 are the fluctuations of the complexity factor $\pm\langle q^2-\langle q^2\rangle\rangle^{1/2}$. A significant increase in these fluctuations is seen at the crossover. We find that these large fluctuations are correlated with the occurrence of peculiar phase distributions around $n=1.8$, such as the one shown in the inset of Fig. 1 for $n=1.85$. Two narrow peaks are distinctly seen in the phase distribution at 0.94π and 1.06π. The spatial distributions of the phase for values comprised in a $\pi/10$ window around each of these two peaks are shown in Figs. 3(a) and 3(b). These two distributions delimitate two distinct spatial regions associated with standing components of the mode, which oscillate at the eigenfrequency of the mode but with a phase lag $\delta\phi=0.12\pi$. This phase lag suggests that this mode results from the coupling between two distinct modes localized on each of the regions of Fig. 3. This would be the analog of the symmetric or antisymmetric solution to the coupled oscillator problem in the presence of leakage which introduces a phase lag different from 0 or π between the components of the hybridized mode. To identify each of the two components of the double-peaked mode of Fig. 1 ($n=1.85$), we remove a scatterer in a spot where the field is high in one of the two regions displayed in Fig. 3 to selectively separate the two contributions. Each perturbed system is excited at the resonant frequency of the original unperturbed mode. The corresponding field distributions are shown in Figs. 4(a) and 4(b). They reproduce the local features of each peak of the mode of Fig. 1, but extend far beyond. The corresponding phase distributions are now single peaked. Note that layers of randomly distributed scatterers (not shown) were added at the boundaries of the perturbed system in order to increase the lifetime of the mode of Fig. 4(a), which would be impossible to excite otherwise due to its strong leakage. The resemblance between the normalized original mode Ψ and the normalized complex linear combination of the two modes of Fig. 4, $\Psi_t=\alpha\Psi_a+e^{i\phi}\Psi_b$, is measured by the spatial cross correlation, $\int\int|\Psi||\Psi_t|d^2\vec{r}$, which is equal to 91% for $\alpha=0.78$ and $\phi=0.66\pi$. The two quasimodes composing the double-peaked state have also been identified by introducing gain in the perturbed systems. The wavelengths of the corresponding lasing modes are $\lambda_a=447.9$ nm and $\lambda_b=446.8$ nm, to be compared with $\lambda=447.1$ nm (Fig. 1) for the original state. The linewidths of the passive modes are, respectively, $\delta\lambda_a=1.0$ nm, $\delta\lambda_b=0.6$ nm, and $\delta\lambda=0.8$ nm. The corresponding spreading factors are $\eta_a=0.36$, $\eta_b=0.29$, and $\eta=0.45$. This supports the picture of two coupled quasimodes with distinct wavelengths, overlapping both spectrally and spatially, to form a hybridized double-peaked state. All other identified multipeaked quasimodes [27] (about 50% of the modes) arise around $n=1.85$, in the vicinity of the crossover.

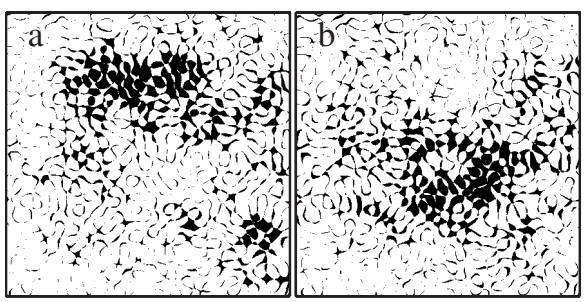

FIG. 3. Binary plots showing in black where the phase is valued (a) between 0.89π and 0.99π and (b) between 1.01π and 1.11π, i.e., two narrow phase ranges around the two peaks at 0.94π and 1.06π seen in phase distribution in the inset of Fig. 1 for $n=1.85$.

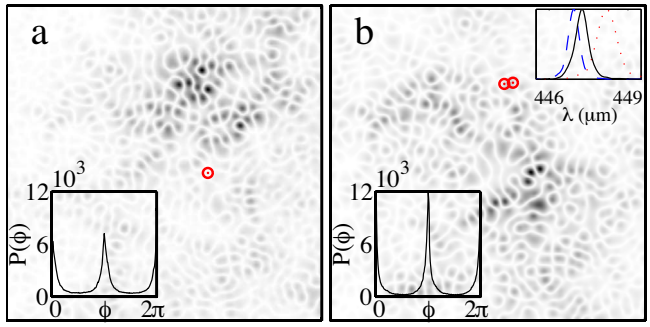

FIG. 4. (Color online) Spatial distribution of the magnitude of the quasimodes together with their phase distribution (lower insets) for two different local perturbations of the original random system of Fig. 1 for $n=1.85$. The locations of the removed scatterers are shown by the circles. Upper inset: spectral lines of modes (a) (dots), (b) (dashed line), and mode $n=1.85$ in Fig. 1 (full line). Wavelengths and linewidths of the modes are given in the text.

These multipeaked states are analogous to necklace states recently observed in nominally localized optical [28] and microwave [29] one-dimensional (1D) layered systems.

Modes overlapping both in space and frequency may couple and form multipeaked extended states even in the localized regime [30]. Although scarce, they are predicted to play an outsized role in transport [31] in contrast to isolated localized states [32]. This is to be compared with the filamentlike fractal picture of the modes at the transition suggested by Aoki [33]. Pendry [31] argued that the picture of 1D necklace states should generalize to 2D and three-dimensional localized random media. However, besides earlier calculations in a percolation model, no observations of necklace states for classical waves in dimensions larger than 1 were reported [34,35]. Our results point out to the existence of necklace states in 2D and show that they should occur preferentially at the transition.

In conclusion, our numerical simulations provide with a detailed description of the quasimodes of open 2D random systems ranging from weakly scattering to strongly localized systems in terms of their spatial extension, but also in terms of their complexity factor. We find multipeaked quasimodes in the vicinity of a well-marked crossover between localized and extended states. Two mechanisms, which may coexist, were proposed to describe the transition [36]. The first one is a gradual spatial expansion of the mode as scattering strength is diminished, with a progressive increase in the localization length. Our results suggest a second mechanism, analogous to a percolation process, where the coupling of localized states lead to extended structures that form necklace states [37–39].

We thank D. Savin, O. Legrand, and F. Mortessagne for fruitful discussions. This work was supported by the Centre National de la Recherche Scientifique (PICS Grant No. 2531 and PEPS Grant No. 07-20) and the Groupement de Recherches IMCODE.

[1] D. J. Thouless, Phys. Rev. Lett. **39**, 1167 (1977).
[2] E. Abrahams, P. W. Anderson, D. C. Licciardello, and T. V. Ramakrishnan, Phys. Rev. Lett. **42**, 673 (1979).
[3] J. Billy *et al.*, Nature (London) **453**, 891 (2008).
[4] G. Roati *et al.*, Nature (London) **453**, 895 (2008).
[5] H. Hu, A. Strybulevych, J. H. Page, S. E. Skipetrov, and B. A. van Tiggelen, Nat. Phys. **4**, 945 (2008).
[6] Z. Q. Zhang, A. A. Chabanov, S. K. Cheung, C. H. Wong, and A. Z. Genack, Phys. Rev. B (to be published); e-print arXiv:0710.3155.
[7] M. Störzer, P. Gross, C. M. Aegerter, and G. Maret, Phys. Rev. Lett. **96**, 063904 (2006).
[8] S. E. Skipetrov and B. A. van Tiggelen, Phys. Rev. Lett. **96**, 043902 (2006).
[9] A. M. García-García, Phys. Rev. Lett. **100**, 076404 (2008).
[10] See H. Cao, Waves Random Media **13**, R1 (2003), and references therein.
[11] K. L. van der Molen, R. W. Tjerkstra, A. P. Mosk, and A. Lagendijk, Phys. Rev. Lett. **98**, 143901 (2007).
[12] S. M. Dutra and G. Nienhuis, Phys. Rev. A **62**, 063805 (2000).
[13] R. Pnini and B. Shapiro, Phys. Rev. E **54**, R1032 (1996).
[14] Y. H. Kim, U. Kuhl, H. J. Stockmann, and P. W. Brouwer, Phys. Rev. Lett. **94**, 036804 (2005).
[15] A. Taflove, *Computational Electrodynamics: The Finite-Difference Time-Domain Method* (Artech House, Norwood, 1995).
[16] J. P. Berenger, J. Comput. Phys. **114**, 185 (1994).
[17] C. Vanneste, P. Sebbah, and H. Cao, Phys. Rev. Lett. **98**, 143902 (2007).
[18] A. E. Siegman, *Lasers* (University Science Books, Mill Valley, 1986).
[19] P. Sebbah and C. Vanneste, Phys. Rev. B **66**, 144202 (2002).
[20] H. Kogelnik and C. V. Shank, J. Appl. Phys. **43**, 2327 (1972).
[21] X. Wu, W. Fang, A. Yamilov, A. A. Chabanov, A. A. Asatryan, L. C. Botten, and H. Cao, Phys. Rev. A **74**, 053812 (2006).
[22] O. I. Lobkis and R. L. Weaver, J. Acoust. Soc. Am. **108**, 1480 (2000).
[23] P. W. Brouwer, Phys. Rev. E **68**, 046205 (2003).
[24] D. V. Savin, O. Legrand, and F. Mortessagne, Europhys. Lett. **76**, 774 (2006).
[25] D. Laurent, O. Legrand, P. Sebbah, C. Vanneste, and F. Mortessagne, Phys. Rev. Lett. **99**, 253902 (2007).
[26] Note that these results also confirm and extend for all regimes of scattering the essential role of the natural resonances of the passive system in random lasing, which has been recently debated in [11] and V. M. Apalkov, M. E. Raikh, and B. Shapiro, Phys. Rev. Lett. **89**, 016802 (2002); S. Mujumdar, M. Ricci, R. Torre, and D. S. Wiersma, *ibid.* **93**, 053903 (2004); X. Wu and H. Cao, Phys. Rev. A **77**, 013832 (2008); H. E. Türeci, L. Ge, S. Rotter, and A. D. Stone, Science **320**, 643 (2008).
[27] See EPAPS Document No. E-PLRAAN-79-R01904 for an example of a three-peak necklace state. For more information on EPAPS, see http://www.aip.org/pubservs/epaps.html
[28] J. Bertolotti, S. Gottardo, D. S. Wiersma, M. Ghulinyan, and L. Pavesi, Phys. Rev. Lett. **94**, 113903 (2005).
[29] P. Sebbah, B. Hu, J. M. Klosner, and A. Z. Genack, Phys. Rev. Lett. **96**, 183902 (2006).
[30] K. Y. Bliokh, Y. P. Bliokh, V. Freilikher, A. Z. Genack, and P. Sebbah, Phys. Rev. Lett. **101**, 133901 (2008).
[31] J. B. Pendry, J. Phys. C **20**, 733 (1987); J. B. Pendry, Adv. Phys. **43**, 461 (1994).
[32] M. Ya. Azbel, Solid State Commun. **45**, 527 (1983).
[33] H. Aoki, J. Phys. C **16**, L205 (1983).
[34] Z. Q. Zhang and P. Sheng, Phys. Rev. B **44**, 3304 (1991).
[35] I. Dasgupta, T. Saha, and A. Mookerjee, Phys. Rev. B **47**, 3097 (1993).
[36] J. J. Ludlam, S. N. Taraskin, S. R. Elliott, and D. A. Drabold, J. Phys.: Condens. Matter **17**, L321 (2005).
[37] P. Sheng, Science **313**, 1399 (2006).
[38] J. Pendry, Physics **1**, 20 (2008).
[39] This is in contrast with the percolation model of Anderson localization described by D. J. Thouless, Phys. Rep., Phys. Lett. **13**, 93 (1974), which is only relevant for electronic waves in a random potential. For classical waves in dielectric random media, the energy of the equivalent quantum particle is always positive and above a disordered potential consisting of negative wells embedded in a zero potential. See, for instance, A. Lagendijk and B. A. Van Tiggelen, *ibid.* **270**, 143 (1996).